Calcium Transport of *Plasmodium chabaudi*-infected Erythrocytes

KAZUYUKI TANABE, ROSS B. MIKKELSEN, and DONALD F. H. WALLACH
Tufts-New England Medical Center, Therapeutic Radiology Department, Radiobiology Division, Boston, Massachusetts 02111

ABSTRACT The calcium content and transport processes of *Plasmodium chabaudi*-infected rat erythrocytes were analyzed by atomic absorption spectroscopy and $^{45}Ca^{2+}$ flux measurements. Infected erythrocytes, after fractionation on metrizamide gradients according to stage of parasite development, exhibited progressively increasing levels of Ca^{2+} with schizont and gametocytes containing 10- to 20-fold greater calcium levels than normal cells (0.54 ± 0.25 nmol/10^8 cells). $^{45}Ca^{2+}$ flux experiments showed both increased influx and decreased efflux in infected erythrocytes. Tris/NH_4Cl lysis of normal erythrocytes preloaded with $^{45}Ca^{2+}$ with the Ca^{2+} ionophore A23187 released >90% of cell calcium after incubation in ethyleneglycol bis(aminoethylether) *N,N'*-tetraacetic acid containing buffer, whereas lysis of the infected erythrocyte membrane resulted in release of 10–20% cell Ca^{2+}, with the remaining portion associated with the isolated parasite fraction. This information together with the effects of various metabolic inhibitors indicates the presence of a parasite Ca^{2+} compartment in *P. chabaudi*-infected erythrocytes.

Dicyclohexylcarbodiimide (DCCD) an inhibitor of proton ATPases of chloroplasts, bacteria, yeast, and mitochondria, and the proton ionophore, carbonyl cyanide *m*-chlorophenylhydrazone (CCCP), inhibited Ca^{2+} influx and stimulated efflux from infected cells. These results combined with evidence for a DCCD- and CCCP-sensitive membrane potential in *P. chabaudi*-infected cells (Mikkelsen et al., accompanying manuscript) suggest that Ca^{2+} transport of intraerythrocytic parasites is coupled to a proton-motive force across the *Plasmodia* plasma membrane.

The calcium ion is an essential component of many cellular regulatory processes, and cells expend considerable energy to maintain low levels of free cytoplasmic Ca^{2+}. In the case of enucleated erythrocytes, low cytoplasmic Ca^{2+} concentrations are achieved by a combination of plasma membrane Ca^{2+} binding, low membrane Ca^{2+} permeability, and active extrusion by Ca^{2+}, Mg^{2+}-ATPase pump (1, 2). Elevation of intracellular Ca^{2+} results in decreased membrane deformability, altered monovalent cation transport, and modification of membrane protein structure, e.g. spectrin degradation (1, 3).

Malaria is a blood-borne disease in which the asexual development of the parasite *Plasmodium* occurs within the host erythrocyte. Few investigators have addressed the general issue of ion transport in *Plasmodium*-infected erythrocytes, although increased osmotic fragility is a common observation of *Plasmodium*-infected erythrocytes. Dunn (4) has shown increased sodium and decreased potassium intracellular levels resulting in part from decreased Na^+, K^+-ATPase activity of parasitized erythrocytes. No information is available concerning Ca^{2+} levels and intracellular Ca^{2+} distribution in infected cells or the relative contributions of erythrocyte and parasite Ca^{2+} transport processes of infected cells. Such information may indicate mechanisms by which the parasite modifies its intracellular environment for optimal growth.

In the present study we have examined the Ca^{2+} content and transport processes of rat erythrocytes infected with *Plasmodium chabaudi*.

MATERIALS AND METHODS

Reagents

Reagents and their respective suppliers were: [^{3}H]polyethylene glycol (4000 mol wt, 2 mCi/gm), $^{45}CaCl_2$ (18.2 mCi/mg) and [^{3}H]H_2O (1 mCi/ml) from New England Nuclear (Boston, MA); SF 1250 silicone oil (General Electric Co., West Point, NY), antimycin A, BSA (fraction-V), CCCP, EGTA, HEPES, NaCN, NaN_3·Tris (Sigma Chemical Co., St. Louis, MO), metrizamide (Nyegaard & Co., Oslo, Norway), DCCD (Aldrich Chemical Co., Metuchen, NJ), A23187 (a gift of

THE JOURNAL OF CELL BIOLOGY · VOLUME 93 JUNE 1982 680-684

Dr. R. L. Hamill, Eli Lilly Laboratories, Indianapolis, IN), and atomic absorbance grade $LaCl_3$ and HCl (Aldrich Chemical Co., Metuchen, NJ).

Cell Preparation

P. chabaudi was originally obtained from Dr. Herbert Cox of Michigan State University and maintained by weekly passage of infected cells in donor male rats (Sprague-Dawley, 6–7 wk, Charles River, Wilmington, MA). Infection of animals and a γ-irradiation procedure to deplete blood of leukocytes and immature erythrocytes have been described (5).

Blood is centrifuged at 700 *g* for 5 min, the serum is discarded, and the residual buffy coat is removed. A 15–20% cell suspension in RPMI 1640 is layered onto a cellulose powder column (6) equilibrated with PBS without Mg^{2+}. After standing for 10 min, cells are eluted with RPMI at 1 ml/min. The cell suspension is free of platelets and immature erythrocytes, and leucocyte contamination is $<10^{-3}$%. Infected erythrocytes are fractionated on metrizamide gradients by modification of the method of Eugui and Allison (7). A stock metrizamide solution of 18.3% (wt/vol) is made with 40% PBS and diluted to appropriate densities as described in Table I.

Measurement of Calcium Content

Cells (10^8) in RPMI are centrifuged through 500 μl of silicone oil at 5,000 g·min in a Beckman microfuge (Beckman Instruments, Palo Alto, CA) to separate cells from the medium. After the silicone oil and medium are aspirated off, the cell pellet is suspended in 0.1% $LaCl_3$, 0.5 M HCl, and the insoluble material is sedimented at 30,000 *g*·min. The supernatant is assayed for Ca^{2+} content with an Instrumentation Laboratory 551 atomic absorption spectrophotometer. Extracellular space Ca^{2+} in the cell pellet is calculated by monitoring the extracellular volume with [^{3}H]polyethylene glycol (8).

Calcium Influx and Efflux

To initiate Ca^{2+} influx, 2×10^9 cells in (10 mM HEPES, pH 7.2, 140 mM NaCl, 5 mM KCl, 5 mM glucose, 1 mM $MgCl_2$) (HBS) are diluted 10-fold with HBS containing various concentrations of Ca^{2+} and 20 μCi $^{45}Ca^{2+}$/ml. At various times of incubation, 100 μl of cells are diluted with 1 ml of ice-cold HBS in a Beckman microfuge tube and immediately washed twice by centrifugation in the microfuge for 5 s. The centrifuge tube tip is cut off directly into polyethylene liquid scintillation vials. Control experiments demonstrated that dilution of cells into ice-cold HBS inhibits both $^{45}Ca^{2+}$ influx and efflux processes of normal and infected cells (e.g. Fig. 1).

To measure Ca^{2+} efflux, cells (2×10^9) in HBS plus 1.0 mM Ca^{2+} and 200 μCi $^{45}Ca^{2+}$/ml are incubated for 30 min at 37°C, washed three times with ice-cold HBS in the microfuge, and diluted 40-fold with HBS at 37°C with or without 0.1 mM EGTA to initiate efflux. Aliquots (200 μl) are withdrawn, washed once with cold HBS, and the pellet is placed into the scintillation vials.

In some experiments, normal erythrocytes are loaded with Ca^{2+} using the divalent cation ionophore A23187. Cells (2×10^9 cells/ml) in HBS are incubated at 37°C with 1 μM A23187 and 0.4–0.5 mM Ca^{2+} (200 μCi/ml $^{45}Ca^{2+}$). After 10 min the cells are washed three times with ice-cold HBS containing 0.5% (wt/vol) bovine serum albumin to remove A23187 (9) and washed an additional three times with HBS.

To determine the distribution of $^{45}Ca^{2+}$ in the parasitized erythrocytes, cells preloaded with $^{45}Ca^{2+}$ are hemolysed with Tris-NH_4Cl (0.75% NH_4Cl, 17 mM Tris HCl, 0.1 mM EGTA, pH 7.4), a method which specifically lyses the erythrocyte membrane but not the parasite (10). 1 vol of the cell suspension is mixed with 19 vol of Tris/NH_4Cl solution. At various times of incubation, samples (200 μl) are taken and washed twice in the microfuge. All the procedures are performed in a cold room (4°C).

RESULTS

Calcium Content of P. Chabaudi-infected Rat Erythrocytes

The differential counts before and after fractionation on metrizamide gradients are shown in Table I. Early parasite stages, ring form-infected erythrocytes, as well as uninfected erythrocytes, are found in the high-density fractions, 4 and pellet. Late stages, schizont and gametocyte, are localized to low-density fractions 1 and 2. Although trophozoite-infected erythrocytes are found in all fractions, microscopic examination showed early trophozoite-infected cells predominantly in fraction 4 and pellet whereas mature trophozoites accumulated in fractions 1–3. All fractions are infective as judged by intraperitoneal infection into normal rats.

Table I also shows results of atomic absorbance Ca^{2+} analyses of the metrizamide fractions of parasite-infected and noninfected erythrocytes. Although the fractionation procedure did not yield absolute separation according to parasite stage, a general trend of increased Ca^{2+} content in late stages with a sharp transition (10-fold increase) at the schizont stage is observed. A comparison of fractions 1 and 2, which are approximately equivalent in relative numbers of schizonts but differ in gametocyte counts, suggests that gametocyte-infected cells maintain a high level of intracellular Ca^{2+}.

Ca^{2+} Transport Measured by $^{45}Ca^{2+}$ Flux and Atomic Absorption

Because the yield of schizont-infected cells is low, a one-step (16.5%, $P = 1.076$) metrizamide gradient is used to fractionate infected erythrocytes into "early" (fractions 4 and pellet) and "late" (fractions 1–3) parasite stages. After separation, cells are washed with Ca^{2+}-free buffer to deplete cells of more than 50% cell Ca^{2+} as judged by atomic absorption analysis.

The results of $^{45}Ca^{2+}$ influx experiments with normal and infected "early" and "late" erythrocytes are shown in Fig. 1. As observed by others (1), normal erythrocytes take up little $^{45}Ca^{2+}$ at 1 mM extracellular Ca^{2+} and 37°C. Cells of the "early" fraction exhibit a slightly greater $^{45}Ca^{2+}$ accumulation than noninfected cells. The real difference in $^{45}Ca^{2+}$ uptake between early parasite and normal erythrocytes is probably greater than observed in these experiments since the infected cell population contains ~50% nonparasitized cells (Table I).

Erythrocytes infected with "late" parasite stages show much

TABLE I

Calcium Content of Plasmodium chabaudi-infected Erythrocytes after Separation of Stages by Metrizamide Gradients

Fraction	Uninfected	Ring form	Trophozoite	Schizont	Gametocyte	Calcium content nmol/10^8 cells ± SE
Infected						
original	51.7	16.2	26.7	5.3	0.1	1.45 ± 0.30
0–12.8% interphase	1.5	1.3	21.5	34.6	41.1	9.61 ± 2.33
12.8–14.6% interphase	3.1	9.1	44.9	39.2	3.7	5.04 ± 0.93
14.6–16.5% interphase	8.1	14.2	51.0	26.7	0	1.96 ± 0.38
16.5–17.8% interphase	36.2	14.6	45.5	3.7	0	1.89 ± 0.43
pellet	53.6	20.1	23.0	3.3	0	1.33 ± 0.18
Normal						0.54 ± 0.25
original						0.64 ± 0.28
17.8% pellet						

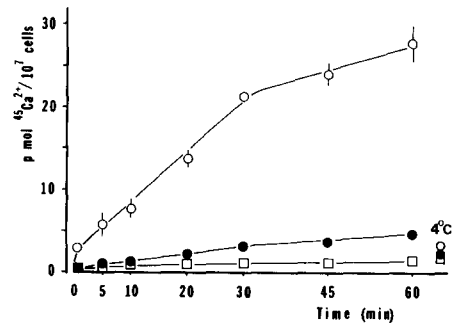

FIGURE 1 $^{45}Ca^{2+}$ influx into late, early, and uninfected erythrocytes. Methods are described in text. Incubation of cells was carried out at 37°C or 4°C (60-min time-point). Late (○——○); early (●——●); uninfected (□——□). Error bars provide range of values for triplicate samples, with equivalent degree of error for early and uninfected cells.

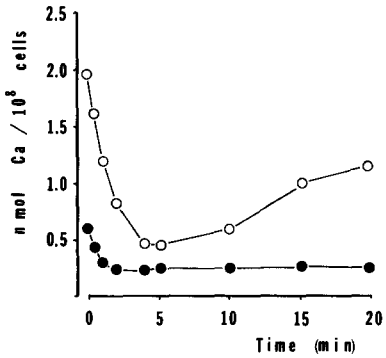

FIGURE 2 Ca^{2+} efflux from normal and infected erythrocytes as measured by atomic absorption spectroscopy. Cells were incubated in HBS plus 1 mM $CaCl_2$ at 37°C for 10 min. At t = 0, aliquots containing 1-5 × 10^8 cells were removed for Ca^{2+} determination. Remaining cells were collected by centrifugation and diluted to a final extracellular Ca^{2+} of 0.025 mM and incubated at 37°C. Cell aliquots were removed at designated times and separated from suspending medium by silicone oil centrifugation. Infected cells were not fractionated by metrizamide gradients, and differential counts were: 51.9 (uninfected), 18.8 (ring), 22.8 (trophozoite), 6.5 (schizont), <0.1 (gametocyte). Measurements performed in triplicate with maximal error between measurements of 20%. Infected (○——○); noninfected (●——●).

enhanced $^{45}Ca^{2+}$ influx. Linear uptake for the first 30 min of incubation of 37°C is followed by a decline in rate of uptake that is probably the consequence of equilibration. The increased $^{45}Ca^{2+}$ uptake is temperature sensitive with complete inhibition at 4°C, and saturable at >1.0 mM extracellular Ca^{2+} concentration.

For efflux experiments, cells are equilibrated with 1 mM $^{45}Ca^{2+}$ for 30 min. When $^{45}Ca^{2+}$-loaded infected cells are diluted 40-fold from 1 mM to 0.025 mM extracellular $^{45}Ca^{2+}$ at 37°C, the cells are depleted of ~40% cell $^{45}Ca^{2+}$ within 5 min but with further incubation they reaccumulate $^{45}Ca^{2+}$ to 70–90% of original cell $^{45}Ca^{2+}$. Total Ca^{2+} efflux as checked by atomic absorption parallels that observed with $^{45}Ca^{2+}$ flux experiments. Thus, infected cells upon 40-fold dilution are depleted of ~70% cell Ca^{2+} within 5 min and then reaccumulate Ca^{2+} to 60% of original cell Ca^{2+} (Fig. 2). The parallel findings obtained with $^{45}Ca^{2+}$ and the atomic absorbance measurements indicate the presence of a Ca^{2+} compartment within infected, but not normal erythrocytes.

In subsequent efflux experiments, $^{45}Ca^{2+}$-loaded normal and infected cells are washed at 4°C and diluted into HBS containing 0.1 mM EGTA, as extracellular Ca^{2+} sink. Since the rate of Ca^{2+} efflux from normal erythrocytes is dependent on intracellular Ca^{2+} levels (11), the cytosolic Ca^{2+} concentration of normal erythrocytes is adjusted by prior incubation with the Ca^{2+} ionophore A23187 at desired extracellular Ca^{2+} concentration.

Fig. 3 shows a semilogarithmic representation of Ca^{2+} efflux from normal and late-stage parasite-infected cells. The rates of efflux from normal erythrocytes at initial intracellular $^{45}Ca^{2+}$ levels of 35.0 and 9.6 picomol/10^7 cells are, respectively, 20 and 6 pmol/min. As cell Ca^{2+} decreases with incubation, the rate of efflux also decreases. By 30 min, normal erythrocytes retain between 10 and 17% of initial $^{45}Ca^{2+}$. In contrast, at approximately equivalent $^{45}Ca^{2+}$ levels, Ca^{2+} efflux from infected cells is complete after the first 5 min, with 60% retention of cell $^{45}Ca^{2+}$ at 30 min. The cell-associated $^{45}Ca^{2+}$ is fully exchangeable since 1–10 μM A23187 induces the release of essentially all $^{45}Ca^{2+}$.

$^{45}Ca^{2+}$ Distribution in Infected Erythrocytes (Fig. 4)

Aliquots are taken from $^{45}Ca^{2+}$-equilibrated late-parasite-stage erythrocytes and A23187-$^{45}Ca^{2+}$-loaded normal erythrocytes after incubation at 4°C in Tris-HCl/NH_4Cl and 0.1 mM EGTA. After centrifugation at 10,000 *g*·min for 1 min, the $^{45}Ca^{2+}$ in the cell pellet and the degree of hemolysis (hemoglobin content in supernatant) are determined. Although A23187-treated normal erythrocytes exhibit only 20% lysis at 5 min, >90% of the total preloaded $^{45}Ca^{2+}$ (17.1 ± 1.8 picomol/10^7 cells) is released during this time. Upon complete lysis, only 7% of the $^{45}Ca^{2+}$ is retained in the cell-ghost pellet. In contrast, 99% of the infected cells are lysed in the first 5 min, with 96% of total cell $^{45}Ca^{2+}$ (15.3 ± 0.5 picomol/10^7 cells) found in the parasite pellet. These results suggest that the major portion of cell Ca^{2+} of the infected erythrocytes is localized to the parasite.

Effects of Metabolic Inhibitors on Ca^{2+} Transport (Tables II and III)

Table II shows effects of various metabolic inhibitors on $^{45}Ca^{2+}$ efflux. Antimycin A, CN^- and N_3^- stimulate $^{45}Ca^{2+}$

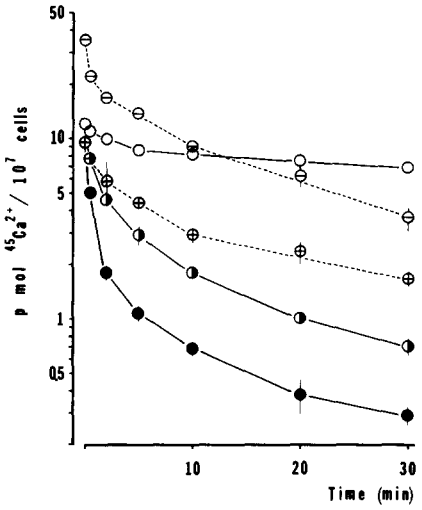

FIGURE 3 $^{45}Ca^{2+}$ efflux from normal and late infected erythrocytes. Methods for A23187 loading of normal erythrocytes and for efflux measurements are described in the text. Infected cells (○-----○); infected cells + 1 μM A23187 (◑-----◑); infected cells +10 μM A23187 (●-----●); normal erythrocytes loaded with A23187 to 35 pmol $^{45}Ca^{2+}$/10^7 cells (⊖-----⊖); normal erythrocytes loaded with A23187 to 9.6 pmol $^{45}Ca^{2+}$/10^7 cells (⊕-----⊕).

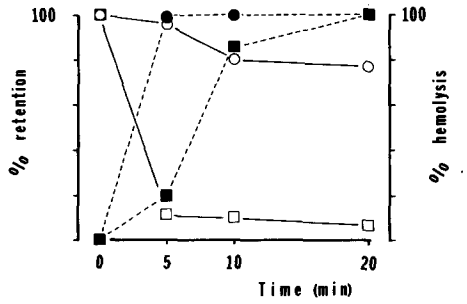

FIGURE 4 $^{45}Ca^{2+}$ levels of infected and normal erythrocytes after Tris/NH_4Cl lysis. Details described in text. Normal erythrocytes were loaded with $^{45}Ca^{2+}$ by the A23187 procedure. $^{45}Ca^{2+}$ contents of normal and late infected cells were, respectively, 17.1 ± 1.8 pmol/10^7 cells and 15.3 ± 0.5 pmol/10^7 cells. Lysis was determined by hemoglobin content in supernatant (absorbance at 410 nm). Normal cells: hemolysis (■-----■); Ca^{2+} retention (□——□). Infected cells: hemolysis (●-----●); Ca^{2+} retention (○——○). Maximal error in measurements was <5%.

TABLE II

Effects of Various Inhibitors on $^{45}Ca^{2+}$ Efflux of P. chabaudi-infected Erythrocytes *

Inhibitor		$^{45}Ca^{2+}$ released (pmol/10^7 cells) at 30 min		
		Infected	Normal	Normal
			A23187 treated	*nontreated*
Control	(t = 30 min)	4.94 ± 0.15 (0)§	7.39 ± 0.10	0.44 ± 0.021
DCCD	100 μM	8.89 ± 0.53 (80)	7.71 ± 0.22	0.45 ± 0.02
	50 μM	8.48 ± 0.19 (72)	7.41 ± 0.21	0.41 ± 0.02
	10 μM	6.33 ± 0.37 (28)	7.38 ± 0.18	0.40 ± 0.02
CCCP	10 μM	8.46 ± 0.14 (71)	7.29 ± 0.21	0.41 ± 0.06
	1 μM	6.50 ± 0.30 (32)	7.27 ± 0.14	0.44 ± 0.06
	0.1 μM	5.48 ± 0.13 (11)	7.33 ± 0.09	0.43 ± 0.03
NaCN	1 mM	6.71 ± 0.19 (36)	7.38 ± 0.07	0.38 ± 0.01
NaN_3	10 mM	6.60 ± 0.29 (34)	7.46 ± 0.04	0.41 ± 0.01
	1 mM	5.16 ± 0.14 (4)	ND	ND
Antimycin A				
	5 μM	6.54 ± 0.68 (32)	7.91 ± 0.09	0.41 ± 0.01
	2 μM	5.79 ± 0.12 (17)	7.37 ± 0.05	ND

* Inhibitors were added at time of dilution of cells into EGTA-containing buffer.
§ Percent relative change.
ND, not determined.

efflux from infected cells by ~30%. A proton ionophore, CCCP (10 μM), also stimulates efflux by 70%. DCCD (50–100 μM), an inhibitor of proton ATPases (12–14), enhances efflux by 70–80%. Kinetic studies show that stimulation of efflux by DCCD (50 μM) and CCCP (10 μM) is complete within 10 min of incubation (data not shown). All inhibitors used have no effect on efflux from normal cells.

The effects of these inhibitors on $^{45}Ca^{2+}$ influx are shown in Table III. Antimycin A, N_3^-, and CCCP inhibit influx into infected cells and decrease $^{45}Ca^{2+}$ levels of normal cells after prolonged incubation (60 min). NaCN reduces $^{45}Ca^{2+}$ accumulation by normal but not infected cells. In contrast, DCCD blocks influx into infected cells by >70%, but with no effect on normal erythrocyte Ca^{2+} influx.

The substantial inhibition of influx by CCCP or DCCD may be secondary to an enhanced net efflux, since little apparent influx is observed during the last 30 min (Table III). This question was examined by experiments in which infected cells are equilibrated with $^{45}Ca^{2+}$ in the presence of 50 μM DCCD (or 10 μM CCCP), washed, and efflux is initiated in the presence of absence of the inhibitor. Results show no stimulation of efflux by DCCD or CCCP. Thus, DCCD and CCCP inhibit $^{45}Ca^{2+}$ uptake as well as stimulate $^{45}Ca^{2+}$ efflux from infected cells.

DISCUSSION

Atomic absorption measurements demonstrate that rat erythrocytes infected with *P. chabaudi* contain elevated levels of Ca^{2+} relative to normal erythrocytes. Enhanced Ca^{2+} levels are observed for all stages of parasite development but the greatest increases occur in post-trophozoite stages. Transport experiments with $^{45}Ca^{2+}$ and by atomic absorbance have shown that both increased Ca^{2+} influx and reduced efflux contribute to the elevated Ca^{2+} levels of infected erythrocytes. From these findings issue several questions concerning intraerythrocytic localization, erythrocyte membrane Ca^{2+} permeability and Ca^{2+}, Mg^{2+}-ATPase activity, and regulation of intraparasite Ca^{2+}.

With respect to intraerythrocytic distribution, two lines of evidence indicate that most of the Ca^{2+} is parasite associated. Tris-NH_4Cl lysis of normal erythrocytes results in the release of 95% of cell Ca^{2+} whereas similar treatment of infected cells causes the release of only 10–20% of the cell Ca^{2+} into the supernatant, with the remainder separating into the parasite pellet. Experiments with metabolic inhibitors are also consist-

TABLE III

Effects of Various Inhibitors of $^{45}Ca^{2+}$ Influx into P. chabaudi-infected Erythrocytes

Inhibitors		Ca^{2+} taken up (pmol/10^7 cells)			
		Infected		Normal	
		30 min	*60 min*	*30 min*	*60 min*
Control		21.5 ± 1.3	30.5 ± 0.9	1.11 ± 0.11	1.71 ± 0.09
DCCD	100 μM	9.9 ± 0.6	10.1 ± 9.1	1.09 ± 0.06	1.57 ± 0.15
	50 μM	12.4 ± 0.5	11.9 ± 0.8	1.13 ± 0.16	1.66 ± 0.25
	10 μM	20.0 ± 0.8	28.3 ± 1.3	1.26 ± 0.04	1.83 ± 0.49
CCCP	10 μM	11.7 ± 1.6	13.2 ± 1.7	0.88 ± 0.04	0.87 ± 0.06
	1 μM	13.7 ± 1.0	20.8 ± 1.1	0.95 ± 0.05	1.07 ± 0.02
	0.1 μM	19.1 ± 1.7	31.7 ± 2.0	1.21 ± 0.13	1.73 ± 0.01
NaCN	1 mM	20.3 ± 0.4	29.0 ± 0.9	1.26 ± 0.14	1.34 ± 0.06
NaN_3	10 mM	15.1 ± 1.0	19.2 ± 0.5	1.07 ± 0.07	1.26 ± 0.11
Antimycin A					
	5 μM	12.9 ± 1.1	22.0 ± 0.9	1.00 ± 0.18	0.84 ± 0.02
	2 μM	17.6 ± 0.8	29.3 ± 3.5	1.13 ± 0.87	1.37 ± 0.08

ent with a parasite Ca^{2+} compartment. DCCD, CCCP, antimycin A, CN^-, and N_3^- are not known to alter ATP production in enucleate erythrocytes and are without effect on Ca^{2+} efflux from $^{45}Ca^{2+}$-equilibrated normal erythrocytes. In contrast, Ca^{2+} efflux is enhanced 30–80% in the case of $^{45}Ca^{2+}$-loaded parasitized erythrocytes, suggesting an energy-dependent retention of Ca^{2+}.

Ca^{2+} accumulation by normal erythrocytes is, however, inhibited 25 to 50% with CCCP, N_3^-, antimycin A, and CN; but not DCCD. The mechanisms for this inhibition are not known, but CCCP and antimycin A are lipophilic and may modify erythrocyte membrane Ca^{2+} permeability as do anesthetics (e. g., see reference 15). Both CN^- and N_3^- bind to hemoglobin and, as has been shown with sickle cell anemia, an altered hemoglobin structure may modify ion permeability of erythrocyte membranes.

With this reservation in mind, some statements concerning regulation of parasite Ca^{2+} can be made. The mitochondrion is a major sink for intracellular Ca^{2+} in most nonmuscle nucleated cells (16). Mitochondrial Ca^{2+}-uptake is energy dependent, being fueled by either mitochondrial ATP or electron transport. Little is nown about mitochondria of intraerythrocytic *Plasmodia*. Except for those in gametocytes, mammalian plasmodial mitochondria are acristate and lack some tricarboxylic acid cycle enzymes (17). Oxygen consumption by parasites, while measurable, is of uncertain significance since schizonts develop in anaerobic tissues (17). Although circumstantial, the evidence suggests that *Plasmodia* mitochondria are ill-equipped to directly participate in concentrating Ca^{2+}.

What is the significance of the Ca^{2+} efflux experiments in which metabolic inhibitors known to block Ca^{2+} transport in mitochondria are used? The parasite populations analyzed have an appreciable number of gametocytes (0.1% to 9.9% in late-stage fractions). Thus, the ~35% enhanced $^{45}Ca^{2+}$ efflux observed with CN^-, N_3^-, and antimycin A may reflect the action of these inhibitors on cristate mitochondrial Ca^{2+} transport or ATP production necessary for Ca^{2+} transport at other subcellular sites. This explanation does not completely account for all energy-dependent Ca^{2+} transport. The degree of stimulation of $^{45}Ca^{2+}$ achieved with DCCD and CCCP, whose sites of action are not necessarily mitochondrial, differs quantitatively from that obtained with CN^-, N_3^-, or antimycin A. Furthermore, an increase in Ca^{2+} uptake is observed in some preparations of infected cells with <0.1% gametocyte (Fig. 2).

In the accompanying paper, evidence for a negative inside membrane potential across *Plasmodia* plasma membrane that is collapsed at low concentrations of CCCP and DCCD is provided. We suggest that this membrane potential is in part the result of an electrogenic H^+-ATPase by analogy with bacteria and yeast (12, 18). On the basis of the Ca^{2+} efflux experiments with DCCD and CCCP, we propose that Ca^{2+} transport of these cells is coupled to the proton motive force across the parasite membrane. Precedent for this proposal comes from work with other eucaryotic unicellular organisms. Stroobant et al. (19) have provided evidence that Ca^{2+} transport across *Neurospora crassa* plasma membranes is coupled to an electrogenic proton-translocating ATPase and involves a Ca^{2+}/H^+ antiporter and transmembrane pH gradient.

A final question which our experimentation indirectly addresses concerns the Ca^{2+} transport processes of the host-cell plasma membrane. Our results showing a parasite Ca^{2+} compartment imply that host-cell mechanisms for maintaining low intracellular Ca^{2+} levels have been modified by the parasite. The enhanced Ca^{2+} uptake by infected cells (Figs. 1 and 2) suggests that the erythrocyte membrane of infected cells may be more permeable to Ca^{2+} or that the Ca^{2+}, Mg^{2+}-ATPase that gates efflux from erythrocytes is inoperative. We are presently investigating Ca^{2+} transport processes of isolated erythrocyte membrane vesicles from *Plasmodium*-infected and normal erythrocytes to resolve this issue.

This work was supported by a National Institutes of Health grant (AI 16087) to R. B. Mikkelsen.

Received for publication 5 August 1981, and in revised form 7 December 1981.

REFERENCES

1. Lew, V. L., and H. G. Ferreira. 1978. Calcium transport and the properties of a calcium-activated potassium channel in red cell membranes. *Curr. Top. Memb. Transport.* 10:217–277.
2. Schatzman, H. F. 1975. Active calcium transport and Ca^{2+}-activated ATPase in human red cells. *Curr. Top. Memb. Transport.* 6:125–168.
3. Anderson, D. R., J. L. Davis, and K. L. Carraway. 1977. Calcium-promoted changes of the human erythrocyte membrane. Involvement of spectrin, transglutaminase, and a membrane-bound protease. *J. Biol. Chem.* 252:6617–6623.
4. Dunn, M. J. 1969. Alterations of red blood cell sodium transport during malarial infection. *J. Clin. Invest.* 48:674–684.
5. Tanabe, K., R. Schmidt-Ullrich, R. B. Mikkelsen, and D. F. H. Wallach. 1982. γ-irradiation as a method to remove leukocytes and polychromatophilic erythrocytes in *Plasmodium chabaudi* infected rats. *J. Parasit.* In press.
6. Richards, W. H. G., and S. G. Williams. 1972. The removal of leucocytes from malaria infected blood. *Ann. Trop. Med. Parasitol.* 67:249–250.
7. Eugui, E. M., and A. C. Allison. 1979. Separation of erythrocytes infected with murine malaria parasites in metrizamide gradients. *Parasitol.* 79:267–275.
8. Mikkelsen, R. B., and B. Koch. 1981. Thermosensitivity of the membrane potential of normal and SV40-transformed hamster lymphocytes. *Cancer Res.* 41:209–215.
9. Sarkadi, B., I. Szasz, and G. Gardos. 1976. The use of ionophores for rapid loading of human red cells with radioactive cations for cation-pump studies. *J. Membr. Biol.* 26:357–370.
10. Martin, W. J., J. Finerty, and A. Rosenthal. 1971. Isolation of *Plasmodium*-berghei (Malaria) parasites by ammonium chloride lysis of infected erythrocytes. *Nature, New Biol.* 233:260–261.
11. Sarkadi, B., I. Szasz, A. Gerloczi, and G. Gardose. 1977. Transport parameters and stoichiometry of active calcium non extrusion in intact human red cells. *Biochim. Biophys. Acta.* 464:93–107.
12. Koslov, I. A., and V. P. Skulachev. 1977. H^+-adenosine triphosphatase and membrane energy coupling. *Biochim. Biophys. Acta.* 463:29–89.
13. Sebold, W. 1977. Biogenesis of mitochondrial ATPase. *Biochim. Biophys. Acta.* 463:1–27.
14. Shoshan, V., and B. R. Selman. 1980. The interaction of N,N'-dicyclohexylcarbdiimide with chloroplast coupling factor 1. *J. Biol. Chem.* 255:384–389.
15. Seeman, P. 1972. Membrane actions of anesthetics and tranquilizers. *Pharmacol Rev.* 24:583–655.
16. Bygrave, F. L. 1978. Mitochondria and the control of intracellular calcium. *Biol. Rev.* 53:43–79.
17. Sherman, I. W. 1979. Biochemistry of *Plasmodium* (Malarial parasites). *Microbiol. Rev.* 43:453–495.
18. Dufour, J-P., B. M. Boutry, and A. Goffeau. 1981. Plasma membrane ATPase of yeast. *J. Biol. Chem.* 255:5735–5741.
19. Stroobant, P., J. B. Dame, and G. A. Scarborough. 1980. The *Neurospora* plasma membrane Ca^{2+} pump. *Fed. Proc.* 39:2437–2441.